

# From 2D Portraits to 3D Realities: Advancing GAN Inversion for Enhanced Image Synthesis

Wonseok Oh\*  
Electrical and Computer Engineering  
University of Michigan  
okong@umich.edu

Youngjoo Jo\*  
ETRI  
run.youngjoo@etri.re.kr

## Abstract

*Image synthesis using StyleGAN has shown remarkable results in 2D portrait image generation. The works of the GAN inversion to manipulate the real image using StyleGAN latent space also show remarkable achievements. 2D GAN inversion has successfully manipulated global attributes such as facial expressions and gender. However, preserving the hairstyle and identity was difficult according to the pose change. We introduce the 3D GAN inversion encoder to make a high-resolution 3D image based on the Geometry Aware 3D Generative Adversarial Network, known as EG3D, which allows explicit control over the pose of the real image subject with multi-view consistency. Our network projects the single 2D portrait images to novel latent space for 3D GAN inversion for the tri-plane of EG3D. We also present multi-view cycle loss, which aims to increase multi-view consistency. By leveraging the new latent space and loss for 3D GAN inversion, our network can successfully convert 2D portrait images into 3D fast.*

## 1. Introduction

Generative Adversarial Networks (GANs) have been actively studied thanks to their ability to synthesize images of high visual quality and diversity. In particular, StyleGANs [18–20] have shown that they effectively encode semantic information in latent space beyond phenomenal results and fidelity in numerous areas of generating and manipulating 2D portrait images. An operation using these characteristics showed promising results in the synthetic image generated by StyleGAN. The GAN inversion is required to apply the operation to the real image. The GAN inversion method converts a specified physical image into a latent space of a pre-trained StyleGAN. This GAN Inversion method has suggested  $\mathcal{W}$  and its extension,  $\mathcal{W}+$  [1] space, depending on the shape of the target latent space for converting.

\*Equal contribution.



Figure 1. Given the desired input image, our framework learned how to find appropriate latent code to achieve accurate image reconstruction in the latent space of a 3D GAN. That way, real images can be quickly converted into 3D images.

Previous studies have mapped a target real image to the corresponding latent code through learning-based methods [3, 28, 34] and optimization-based methods [1, 19, 29]. In terms of reconstruction accuracy, optimization-based methods can efficiently perform much better in inverting images without additional configuration, but they are

time-consuming and challenging to utilize for applications. Learning-based methods train encoders to converge targets to suitable latent space using only a single forward pass, so they are faster, but their visual quality is inferior to optimization-based methods. In addition, the quality will vary depending on the shape of the latent space in which the encoder will reverse the image.

These GAN inversion methods showed good performance for 2D GAN. However, as GAN expands, 3D image generation also shows phenomenal results. Specifically, EG3D [5] utilizes tri-plane presentation to create high-definition 3D composite images with fewer parameters. It also demonstrates that the optimization-based method [29] works well for the StyleGAN2-based backbone in EG3D, enabling real-world images to be converted to 3D. However, designing an appropriate training scheme and latent space to convert 2D images to 3D GAN remains challenging.

In this paper, we introduce a novel framework for controllable Image-to-Image 3D translation which is based on geometry-aware 3D Generative Adversarial Network. Our framework converts the actual 2D image using 3D GAN so that it can create the appropriate tri-plane feature for the render who creates the 3D image. This model allows the pull of style vectors with different scales. Our model utilizes a novel latent space,  $\mathcal{W}_{tri}$  so that the learning-based method’s encoder can convert real-world images to 3D GAN feature maps, which have different characteristics from conventional 2D GANs. The tri-plane feature maps for rendering consist of three orthogonal planes, and the encoder creates a latent code that allows the real-world image to focus separately on each plane through the  $\mathcal{W}_{tri}$  space. Finally, the encoder for the super-resolution module is isolated to extract latent code for high-resolution results. The results of 3D GAN differ from those of 2D GAN, which expresses only the visible area because rendering synthesizes multi-view images. Accordingly, if the encoder is trained only with a loss for 2D image restoration like conventional methods, information on the invisible image area for 3D image synthesis may be omitted. Therefore, we trained the encoder by adding a new loss function so that we can extract features for multi-view images. This loss function allows the characteristics of the target image to be well expressed even when the target image is converted to another viewpoint.

Our main contributions are summarized as follows:

- We introduce novel latent space  $\mathcal{W}_{tri}$  and a framework that could make 3D portrait image by learning-based GAN inversion.
- We trained the encoder with new loss functions to create multi-view image characteristics.

## 2. Related Work

### 2.1. GAN Inversion.

With the development of GAN, many studies have emerged to control latent space. Many recent papers have used StyleGANs [18–20] because of its efficient image performance and semantic abundance of latent space. GAN Inversion is a method of extracting the image by pulling out the latent vector and putting it in the generator. GAN Inversion refers to creating a real-world image through latent manipulation by locating the image in a pre-trained GAN’s latent space as corresponding latent code. In general, there are two methods of inversion. First, the optimization-based method directly tunes the parameter of the generator to express the target image. It exhibits high-quality results without additional learnable parameters, but it takes a long time. I2S [1] embeds the image into the extension latent space  $\mathcal{W}+$  of StyleGAN. The authors of StyleGAN2 [19] proposed a method of optimizing the noise map corresponding to each layer of the synthesis network and latent code. PTI [29] performs pivotal tuning in the latent space for real images. It finds the latent code representing the image, then fixes it and fine-tunes the generator to derive the results. Second, learning-based methods train encoders that create latent codes that can represent real images. Although there is a time advantage because a single inference produces results, it usually results in poor visual quality compared to optimization methods. pSp [28] and e4e [34] directly extract the latent vector of  $\mathcal{W}+$  space using the encoder network. It extended the GAN inversion problem to the image-to-image translation problem by changing the input image because only the encoder network needs to be learned. Another study, Restyle [3], also improves visual quality by allowing encoders to modify latent codes repeatedly. Recently, the studies [4, 9] using a hypernetwork that allows the addition of offset to the generator parameter have revealed promising results.

### 2.2. 3D-aware GAN.

Extending 2D generative adversarial networks to 3D settings has also begun to gain momentum. It has evolved from mesh-based approaches [22, 33] to voxel-based GAN [10, 15, 24, 25, 36], which directly extends CNN generators in 2D settings to 3D. However, it is difficult to adapt to high-resolution 3D GAN training due to the high memory requirements of the voxel grid and the computational burden of 3D convolution. Typically, there is NeRF [23] in which position and direction are added to the 2D image together to make the result. NeRF, which is the content of this neural implicit presentation, performs positional encoding using a fully connected layer and provides a new position view as a result. The 3D-aware GAN using this method includes StyleNeRF [13] and CIPS-3D [38]. However, Neural implicit representations use fully connected layers with po-

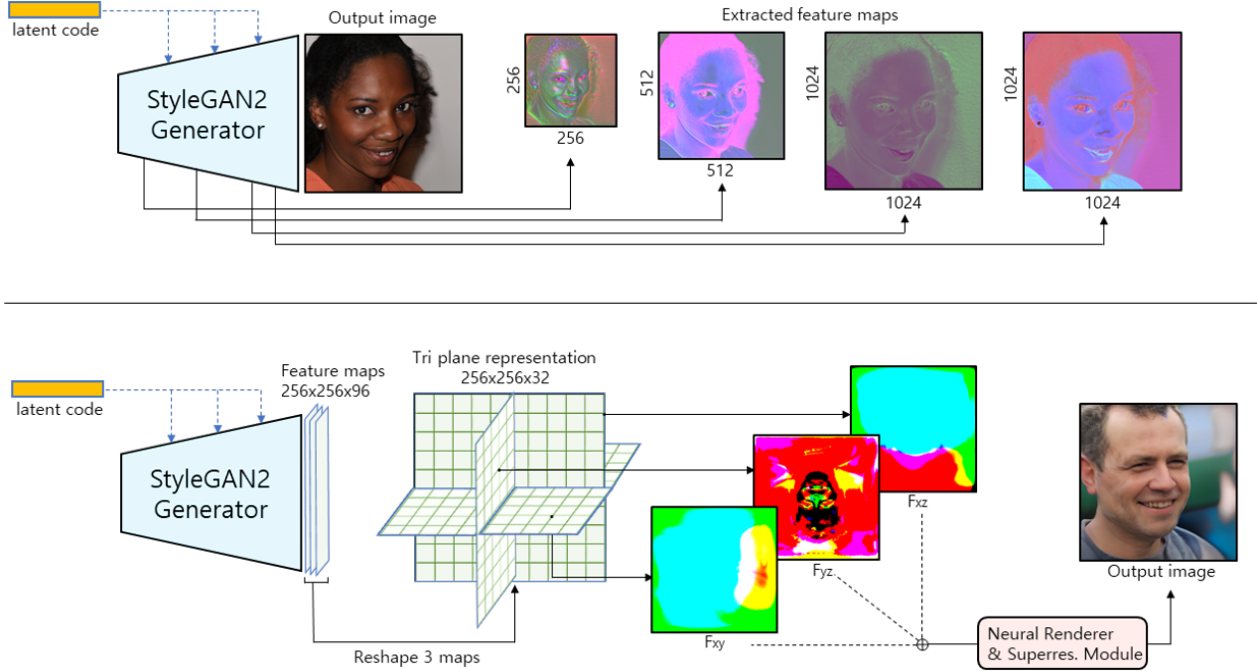


Figure 2. The above is the constructed feature maps with the generator of StyleGAN2 and the extracted feature maps. Below is the image of EG3D with a tri-plane presentation connected to the generator of StyleGAN2. In the case of the StyleGAN2 generator, it can be seen that as the latent code gets closer to the output image, the more it becomes a face shape. On the other hand, it cannot be said that the feature map of EG3D’s triplane has a proper face shape. This is because these feature maps must go through the neural render and Super-resolution module before the output image comes out.

sitional encoding, which can be slow to query. EG3D [5], which we utilize as a 3D generator, does not use conventional inefficient voxel grids. It uses hybrid tri-plane representations because it scales quickly and efficiently with the resolution. It provides greater details for equal capacity for creating high-quality 3D images.

### 2.3. Latent Space Manipulation

The field has recently seen a proliferation of studies that capitalize on StyleGAN’s potential for semantic latent code editing. The intrinsic structure of StyleGAN’s latent space is characterized by a high degree of disentanglement, which has inspired a multitude of methods to investigate semantic latent directions under different levels of supervision. Owing to its finely segregated latent space, StyleGAN has become the framework for these explorations. To uncover these semantic latent directions, the literature offers a panoply of methods. There exist fully-supervised approaches such as [2, 8, 12, 31] which make use of semantic labels, as well as unsupervised methodologies [14, 30, 35] that operate without such labels. Further, innovative techniques [11, 26, 35] have been introduced that utilize the Contrastive Language Image Pre-training (CLIP) model [27] to discover potential directions that facilitate new editing functionalities. However, these techniques have primar-

ily been demonstrated on synthetic images generated within the confines of a pre-trained StyleGAN’s latent space. For generative models that aspire to modify actual real-world imagery, it is imperative to have an effective inversion method that can accurately map these images into the generative latent space.

## 3. Method

### 3.1. Base 3D GAN

The existing 2D CNN-based generator model has limitations in modeling 3D images. This is because there is no information on position when a 2D single image is received as an input. When we visualize the feature map in the process of generating the 2D image as an example of StyleGAN2 [19], which we include in the generator, we can see that a low-resolution coarse-style image comes out at the beginning, and a fine image comes out toward the end. This means that as the input vector flows toward the end, the generator makes the feature map closer to the final image. Therefore, if the image is projected with  $\mathcal{W}+$  space using an encoder, the pose becomes fixed gradually during the generation process. To solve this problem, we mapped latent code into the EG3D [5] network, which enables 3D grounded neural rendering by transforming the feature map

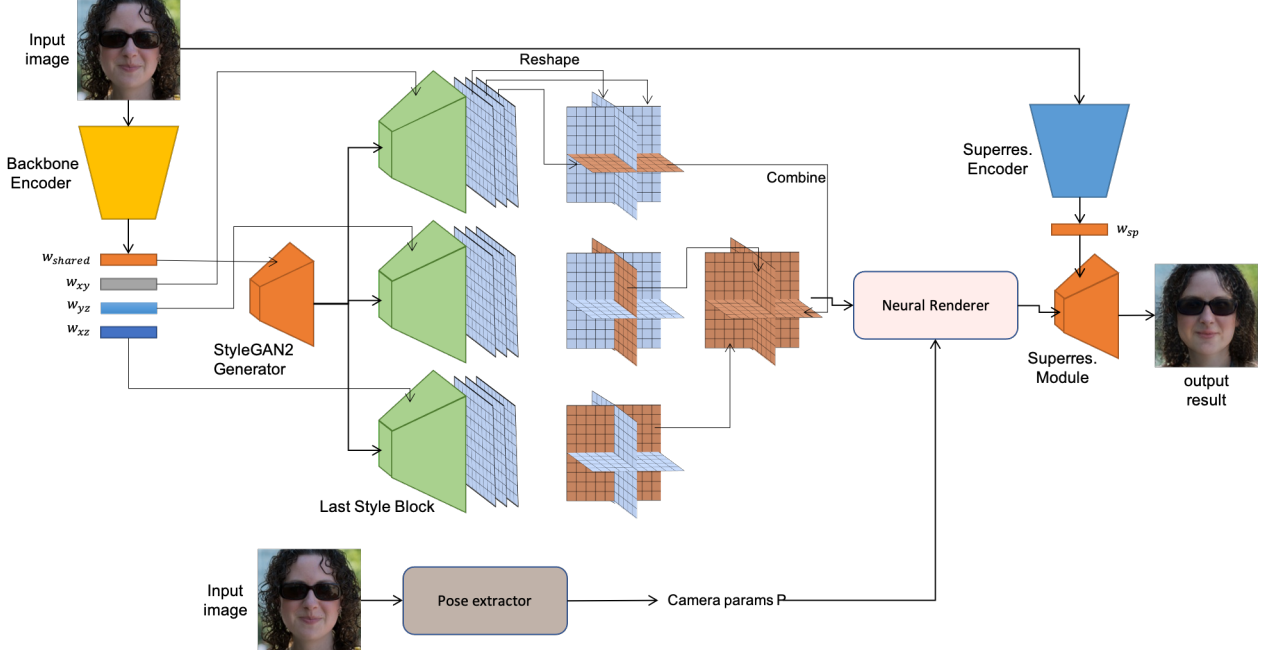


Figure 3. Our framework for converting single portrait photographs into 3D consists of a backbone encoder for neural renders and a super-resolution encoder for super-resolution modules. This architecture establishes a new feature map for rendering at each coordinate. By limiting the area the encoder needs to focus on, our framework can project real images into the latent space of the 3D GAN effectively and quickly.

of StyleGAN2. However, when a 2D image is directly inverted through the encoder network to EG3D with this advantage, the desired form of the 3D image does not come out immediately. The reason is that EG3D reshaped the output feature map of the StyleGAN2 generator into a tri-plane representation by dividing it into three different output feature maps. We visualize the feature maps of 2D and 3D GAN in Figure 2. Visualization of the tri-plane’s three feature maps  $F_{xy}$ ,  $F_{yz}$ , and  $F_{xz}$  with respect to the input image confirms that they are entirely different from the results of the 2D GAN. In 2D GAN, feature maps appear to represent the image’s shape itself, but 3D GAN does not simply represent it. This is because the process of neural rendering for 3D implementation is subsequently continued. Therefore, unlike projecting to 2D generator, we solve this problem by creating a new latent space called  $\mathcal{W}_{tri}$ .

### 3.2. $\mathcal{W}_{tri}$ latent space & Encoder

As described above, the feature maps created by the backbone network of EG3D are distinctive. The EG3D divides the final output of the backbone network into three feature maps  $F_{xy}$ ,  $F_{yz}$ , and  $F_{xz}$  on the channel axis, and the rendering module uses them to synthesize the image. The feature maps for rendering have different characteristics from feature maps in 2D GAN. To embed real images using the encoder, we propose  $\mathcal{W}_{tri}$  latent space that can echo the

characteristics of the orthogonal planes of the tri-plane.

In order to embed the real image to latent space for fitting these feature maps, we use the latent code  $w_{tri} = (w_{shared}, w_{xy}, w_{yz}, w_{xz}, w_{sp})$ . The  $w_{shared}$  code is used as an input to the style blocks of styleGAN2, the backbone network of EG3D.  $w_{xy}$ ,  $w_{yz}$ , and  $w_{xz}$  codes are used to create  $F_{xy}$ ,  $F_{yz}$ , and  $F_{xz}$  planes of tri-plane, respectively. We use  $w_{xy}$ ,  $w_{yz}$ , and  $w_{xz}$  as inputs to the last style block in the backbone network of EG3D. From these three feature maps, we divide them into three by each channel axis for tri-planes, respectively. Extract  $F_{xy}$ ,  $F_{yz}$ , and  $F_{xz}$  planes from each tri-plane and synthesize them to generate the final tri-plane feature maps for rendering. These feature maps will obtain refined orthogonal feature maps optimized for rendering.

EG3D uses the super-resolution module to obtain the conclusive high-resolution image from the raw rendering image. The  $w_{sp}$  code is used as an input to this super-resolution module. Unlike the latent codes of the backbone network, the  $w_{sp}$  code improves the image’s detail for the high-resolution image. This proposed latent space for 3D GAN embedding, which we call  $\mathcal{W}_{tri}$  space, provides the effect of converting a 2D image into 3D with free pose change.

We used Restyle [3] as the basis. Our encoder consists of a super-resolution encoder that makes  $w_{sp}$  code and a

backbone encoder that makes the rest. The super-resolution encoder has the same FPN-based structure as the pSp [28], and the backbone encoder is also composed of an off-the-shelf structure from Restyle (see Figure 3).

### 3.3. Losses

We trained the encoder networks with popular loss in encoder-based methods. It employs a weighted combination of a pixel-wise L2 loss, perceptual loss, identity loss [28], and similarity loss [34] with regularization loss. This loss objective is given by:

$$\begin{aligned}\mathcal{L}_{rec} = & \lambda_2 \mathcal{L}_2 + \lambda_{LPIPS} \mathcal{L}_{LPIPS} \\ & + \lambda_{id} \mathcal{L}_{id} + \lambda_{sim} \mathcal{L}_{sim} + \lambda_{reg} \mathcal{L}_{reg}\end{aligned}\quad (1)$$

$$\mathcal{L}_{reg}(x) = \|E(x) - \bar{w}\|_2 \quad (2)$$

where  $x$  means input image,  $p$  means camera pose parameter of  $x$ ,  $G$  means a EG3D generator,  $E$  means out encoders, and  $\theta$  implies weight.

In order to improve the quality of 3D images, we additionally use pose cycle loss (Equation 3). The dataset of the real-world face has various poses for a person. However, traditional losses in 2D GAN inversion tasks focus on 2D image reconstruction. So, the training performance is insufficient. Since we use 3D GAN, we can change poses through neural rendering. This means that our encoder has to create the same codes from pose-changed images from the fixed latent code. Figure 4 shows our idea that is to randomly pick one from multiple random camera parameters and calculate the cycle code loss. As a result, FFHQ or CelebA-HQ, a given 2D image dataset, lacks the poses of the image (person A does not exist in various poses). Therefore, it is possible to produce the same effect learned from data with various poses per each identity image.

$$\mathcal{L}_{cyc}(x) = \|E(x), E(G(E(x), \hat{p}))\|_1 \quad (3)$$

Finally, the total loss function that combines the above losses is as follows. Each of the lambda values is a hyperparameter that determines the loss weight. Learning can be regulated to the situation while easily changing values.

$$\mathcal{L}_{total} = \mathcal{L}_{rec} + \lambda_{cyc} \mathcal{L}_{cyc} \quad (4)$$

## 4. Experiments

### 4.1. Settings

**Datasets.** We perform an evaluation on a set of face image domains to demonstrate the approach. We use FFHQ datasets for training and CelebA-HQ test sets for evaluation.

**Baseline.** For our approach, we employ the Restyle training process. Therefore, the  $w_{tri}$  latent code is updated repeatedly 5 times through the encoder. To generate the 3D image, we use the pre-trained EG3D framework and fix all parameters of it. We use off-the-shelf face detection Deep3DFaceRecon [7] to extract a 16-size camera extrinsic parameter from test images. We use the same fixed 9-size camera intrinsic parameters from EG3D. For the random identity loss  $\mathcal{L}_{cyc}$ , we randomly extract a camera parameter from 120 aligned camera parameters and use it for each iteration.

### 4.2. Comparison

We first compare our learning-based inversion work with the current state-of-the-art optimization-based technique PTI on EG3D. Although optimization methods for each input image exhibit excellent visual restoration quality results, there is a long computational time cost. In addition, we compare quality and identity preservation according to viewpoint changes with additional first-order-model [32] that are not GAN inversion methods but can create animations with single images. These results show that our framework effectively uses latent spaces suitable for multi-viewpoint 3D-aware synthetic image generation.

**Qualitative Evaluation.** We start with ReStyle, the base model, and begin by showing a qualitative comparison of alternative inversion approaches. Figure 5 shows that our approach to new latent space and loss improves the baseline in terms of quality. However, quality is inferior to optimization-based methods. However, our model can achieve the 3D reconstruction quality with considerably low inference time. We also compare the 3D GAN model with how to warp the image to fit the given pose by utilizing the existing flow map. To generate the image of target poses, we use the average face of the pre-trained EG3D generator and add the camera poses to make different pose images for the same specimen. This method produces good results when there is a lot of video frame information enough to compute the flow map, as shown in Figure 6. It produces results that seem to have only failed to reflect the three-dimensional viewpoints where there will be too many pose changes. In addition, our model can produce results that fit the target pose much more accurately.

	<b>Restyle</b>	<b>Ours</b>	<b>PTI</b>
<b>LPIPS</b> ↓	0.25	0.22	0.10
<b>ID</b> ↑	0.35	0.36	0.57
sec/img	0.54	0.54	457.0

Table 1. Quantitative reconstruction results over the CelebA-HQ [17] test dataset.

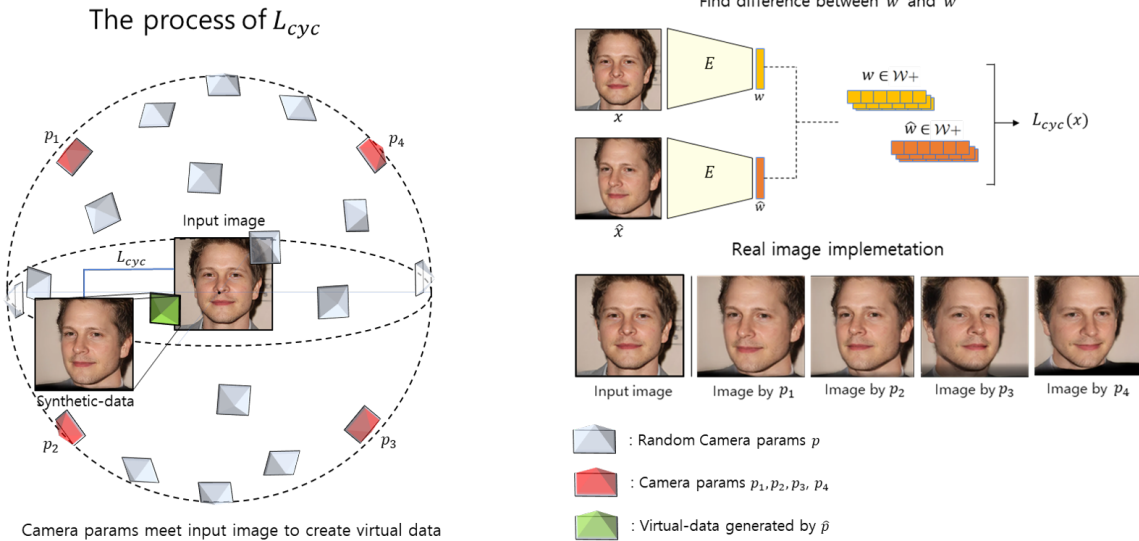


Figure 4. The role of  $\mathcal{L}_{cyc}$  included in a total loss is to create a virtual data creation effect by meeting the camera parameters with a new input image. These results are similar to learning data with pose information in various directions for learning data that lacks pose information. By passing the generated virtual data and input image through the encoder  $E$ ,  $w$  and  $\hat{w}$  are obtained, as shown in the upper right figure. We defined the difference in the generated latent vector present in  $\mathcal{W}^+$  latent space as  $\mathcal{L}_{cyc}$  and trained in the direction of reducing it. The result of the implementation shows that camera parameters at different positions produce output images of various poses for the same input image.

**Quantitative Evaluation.** We compare Restyle baseline and PTI, the latest inversion techniques mentioned above, with our method for quantitative comparison. We apply the commonly-used LPIPS [37] metrics to measure reconstruction and the face recognition method [16] for identity similarity. For the training process of Restyle, we iteratively update  $\mathcal{W}_{tri}$  latent vectors five times. For optimization, we projected 500 steps for a single image to make latent vectors in  $\mathcal{W}^+$  space. Meanwhile, for PTI, 350 pivotal tuning steps are processed. In table 1, we show that our new latent space and loss contribute to the quantitative performance as well as the quality of the baseline. It also offers advantages in the application field because it can create 3D-aware synthetic images much faster, although it is less reproducible than optimization methods. We also showed performance improvement when our proposed method was applied sequentially. This result contains important ablations and gives us various quantitative results related to 3D inversion. As shown in the Table 2,  $\mathcal{W}_{tri}$  has strengths in LPIPS and  $\mathcal{L}_{cyc}$  strengthens ID consistency. To sum up, the result shows that the main contribution of our model, which is expressed by  $\mathcal{W}_{tri}$  and  $\mathcal{L}_{cyc}$  gives a meaningful difference between baseline and would have strengthened the result.

	<b>LPIPS<math>\downarrow</math></b>	<b>ID<math>\uparrow</math></b>
baseline	0.254	0.353
$+\mathcal{W}_{tri}$	0.227	0.352
$+\mathcal{L}_{cyc}$	0.223	0.362

Table 2. Quantitative comparison results between baseline, baseline+  $\mathcal{W}_{tri}$ , and baseline +  $\mathcal{W}_{tri} + \mathcal{L}_{cyc}$

## 5. Conclusions

In this paper, we introduced the 3D GAN inversion encoder to make a high-quality 3D-aware synthetic image using a single 2D image. To improve the quality of inversion, we created a new feature map corresponding to each coordinate and newly designed  $\mathcal{L}_{cyc}$ , which is added to the total loss. By creating a new feature map, the performance of the encoder network was highly improved. The new customized loss,  $\mathcal{L}_{cyc}$ , corrects the error when the 2D image is projected on the new feature map. This  $\mathcal{L}_{cyc}$  was slightly different from the existing cycle consistency loss, which was determined by making latent codes from the image and setting the difference as the loss value. Likewise, when looking at the learning results, it was possible to confirm the quality improvement of the image by correcting

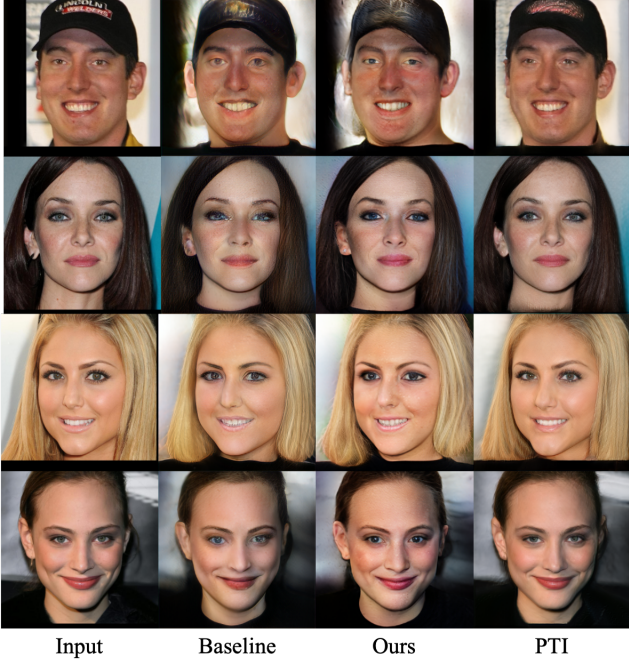


Figure 5. Inversion comparison results. Our approach makes the baseline Restyle [3] even better. However, the optimization-based PTI [29] shows better visual results. Zoom-in is recommended.

the loss. Our method performs a way of inverting real images to 3D GANs, but apart from providing excellent visual quality, there are limitations in expressing the 3D volume of the dataset. In other words, the tendency to create a backbone feature map that depends on the viewpoint the input image views is vital, so reproducibility is sufficient. Still, the rendering volume expression tends to be insufficient. Therefore, the challenge for volume expression is a future task. Since our model is generated from the StyleGAN2 backbone, we can proceed with various application experiments using the StyleGAN2 latent space for future work. This contains the reconstruction of a 2D sketch, 2D semantic mask map using CelebAMask-HQ [21], and various image control methods [11, 26, 35] such as hairstyle and facial expression into 3D. Also, we can use our network to make 3D-aware synthetic images using non-human datasets such as AFHQ Dataset [6]. In summary, to create a 3D portrait image from the 2D image, new feature maps, and loss to correct the feature map were newly presented. Compared with the existing methods, a greater effect was obtained.

## 6. Acknowledgements

This work was supported by Institute of Information & Communications Technology Planning & Evaluation(IITP) grant funded by the Korea government(MSIT) (No.2014-3-00123, Development of High Performance Visual BigData

Discovery Platform for Large-Scale Realtime Data Analysis, No.2022-0-00124, Development of Artificial Intelligence Technology for Self-Improving Competency-Aware Learning Capabilities, and No.RS-2022-00187238, Development of Large Korean Language Model Technology for Efficient Pre-training)



Figure 6. Comparison with pose changes. We compared our method with the warp-based model and the first-order model. The top right images are the target poses, and the top left images are the input images.

## References

- [1] Rameen Abdal, Yipeng Qin, and Peter Wonka. Image2stylegan: How to embed images into the stylegan latent space? In *Proceedings of the IEEE/CVF International Conference on Computer Vision*, pages 4432–4441, 2019. [1](#), [2](#)
- [2] Rameen Abdal, Peihao Zhu, Niloy J Mitra, and Peter Wonka. Styleflow: Attribute-conditioned exploration of stylegan-generated images using conditional continuous normalizing flows. *ACM Transactions on Graphics (ToG)*, 40(3):1–21, 2021. [3](#)
- [3] Yuval Alaluf, Or Patashnik, and Daniel Cohen-Or. Restyle: A residual-based stylegan encoder via iterative refinement. In *Proceedings of the IEEE/CVF International Conference on Computer Vision*, pages 6711–6720, 2021. [1](#), [2](#), [4](#), [7](#)
- [4] Yuval Alaluf, Omer Tov, Ron Mokady, Rinon Gal, and Amit Bermano. Hyperstyle: Stylegan inversion with hypernetworks for real image editing. In *Proceedings of the IEEE/CVF Conference on Computer Vision and Pattern Recognition*, pages 18511–18521, 2022. [2](#)
- [5] Eric R. Chan, Connor Z. Lin, Matthew A. Chan, Koki Nagano, Boxiao Pan, Shalini De Mello, Orazio Gallo, Leonidas Guibas, Jonathan Tremblay, Sameh Khamis, Tero Karras, and Gordon Wetzstein. Efficient geometry-aware 3D generative adversarial networks. In *CVPR*, 2022. [2](#), [3](#)
- [6] Yunjey Choi, Youngjung Uh, Jaejun Yoo, and Jung-Woo Ha. Stargan v2: Diverse image synthesis for multiple domains. In *Proceedings of the IEEE/CVF conference on computer vision and pattern recognition*, pages 8188–8197, 2020. [7](#)
- [7] Yu Deng, Jiaolong Yang, Sicheng Xu, Dong Chen, Yunde Jia, and Xin Tong. Accurate 3d face reconstruction with weakly-supervised learning: From single image to image set. In *Proceedings of the IEEE/CVF Conference on Computer Vision and Pattern Recognition Workshops*, pages 0–0, 2019. [5](#)
- [8] Emily Denton, Ben Hutchinson, Margaret Mitchell, and Timnit Gebru. Detecting bias with generative counterfactual face attribute augmentation. 2019. [3](#)
- [9] Tan M. Dinh, Anh Tuan Tran, Rang Nguyen, and Binh-Son Hua. Hyperinverter: Improving stylegan inversion via hypernetwork. In *Proceedings of the IEEE/CVF Conference on Computer Vision and Pattern Recognition (CVPR)*, 2022. [2](#)
- [10] Matheus Gadelha, Subhransu Maji, and Rui Wang. 3d shape induction from 2d views of multiple objects. In *2017 International Conference on 3D Vision (3DV)*, pages 402–411. IEEE, 2017. [2](#)
- [11] Rinon Gal, Or Patashnik, Haggai Maron, Gal Chechik, and Daniel Cohen-Or. Stylegan-nada: Clip-guided domain adaptation of image generators. *arXiv preprint arXiv:2108.00946*, 2021. [3](#), [7](#)
- [12] Lore Goetschalckx, Alex Andonian, Aude Oliva, and Phillip Isola. Ganalyze: Toward visual definitions of cognitive image properties. In *Proceedings of the IEEE/CVF International Conference on Computer Vision*, pages 1027–1036, 2021. [3](#)

- tional Conference on Computer Vision, pages 5744–5753, 2019. 3
- [13] Jiatao Gu, Lingjie Liu, Peng Wang, and Christian Theobalt. Stylenet: A style-based 3d-aware generator for high-resolution image synthesis. *arXiv preprint arXiv:2110.08985*, 2021. 2
- [14] Erik Härkönen, Aaron Hertzmann, Jaakko Lehtinen, and Sylvain Paris. Ganspace: Discovering interpretable gan controls. *Advances in Neural Information Processing Systems*, 33:9841–9850, 2020. 3
- [15] Peter Hedman, Pratul P Srinivasan, Ben Mildenhall, Jonathan T Barron, and Paul Debevec. Baking neural radiance fields for real-time view synthesis. In *Proceedings of the IEEE/CVF International Conference on Computer Vision*, pages 5875–5884, 2021. 2
- [16] Yuge Huang, Yuhang Wang, Ying Tai, Xiaoming Liu, Pengcheng Shen, Shaoxin Li, Jilin Li, and Feiyue Huang. Curricularface: adaptive curriculum learning loss for deep face recognition. In *proceedings of the IEEE/CVF conference on computer vision and pattern recognition*, pages 5901–5910, 2020. 6
- [17] Tero Karras, Timo Aila, Samuli Laine, and Jaakko Lehtinen. Progressive growing of gans for improved quality, stability, and variation. *arXiv preprint arXiv:1710.10196*, 2017. 5
- [18] Tero Karras, Samuli Laine, and Timo Aila. A style-based generator architecture for generative adversarial networks. In *Proceedings of the IEEE/CVF conference on computer vision and pattern recognition*, pages 4401–4410, 2019. 1, 2
- [19] Tero Karras, Samuli Laine, Miika Aittala, Janne Hellsten, Jaakko Lehtinen, and Timo Aila. Analyzing and improving the image quality of stylegan. In *Proceedings of the IEEE/CVF conference on computer vision and pattern recognition*, pages 8110–8119, 2020. 1, 2, 3
- [20] Tero Karras, Miika Aittala, Samuli Laine, Erik Härkönen, Janne Hellsten, Jaakko Lehtinen, and Timo Aila. Alias-free generative adversarial networks. In *Proc. NeurIPS*, 2021. 1, 2
- [21] Cheng-Han Lee, Ziwei Liu, Lingyun Wu, and Ping Luo. Maskgan: Towards diverse and interactive facial image manipulation. In *Proceedings of the IEEE/CVF Conference on Computer Vision and Pattern Recognition*, pages 5549–5558, 2020. 7
- [22] Yiyi Liao, Katja Schwarz, Lars Mescheder, and Andreas Geiger. Towards unsupervised learning of generative models for 3d controllable image synthesis. In *Proceedings of the IEEE/CVF conference on computer vision and pattern recognition*, pages 5871–5880, 2020. 2
- [23] Ben Mildenhall, Pratul P Srinivasan, Matthew Tancik, Jonathan T Barron, Ravi Ramamoorthi, and Ren Ng. Nerf: Representing scenes as neural radiance fields for view synthesis. In *European conference on computer vision*, pages 405–421. Springer, 2020. 2
- [24] Thu Nguyen-Phuoc, Chuan Li, Lucas Theis, Christian Richardt, and Yong-Liang Yang. Hologan: Unsupervised learning of 3d representations from natural images. In *Proceedings of the IEEE/CVF International Conference on Computer Vision*, pages 7588–7597, 2019. 2
- [25] Thu H Nguyen-Phuoc, Christian Richardt, Long Mai, Yongliang Yang, and Niloy Mitra. Blockgan: Learning 3d object-aware scene representations from unlabelled images. *Advances in Neural Information Processing Systems*, 33:6767–6778, 2020. 2
- [26] Or Patashnik, Zongze Wu, Eli Shechtman, Daniel Cohen-Or, and Dani Lischinski. Styleclip: Text-driven manipulation of stylegan imagery. In *Proceedings of the IEEE/CVF International Conference on Computer Vision*, pages 2085–2094, 2021. 3, 7
- [27] Alec Radford, Jong Wook Kim, Chris Hallacy, Aditya Ramesh, Gabriel Goh, Sandhini Agarwal, Girish Sastry, Amanda Askell, Pamela Mishkin, Jack Clark, et al. Learning transferable visual models from natural language supervision. In *International Conference on Machine Learning*, pages 8748–8763. PMLR, 2021. 3
- [28] Elad Richardson, Yuval Alaluf, Or Patashnik, Yotam Nitzan, Yaniv Azar, Stav Shapiro, and Daniel Cohen-Or. Encoding in style: a stylegan encoder for image-to-image translation. In *IEEE/CVF Conference on Computer Vision and Pattern Recognition (CVPR)*, 2021. 1, 2, 5
- [29] Daniel Roich, Ron Mokady, Amit H Bermano, and Daniel Cohen-Or. Pivotal tuning for latent-based editing of real images. *ACM Trans. Graph.*, 2021. 1, 2, 7
- [30] Yujun Shen and Bolei Zhou. Closed-form factorization of latent semantics in gans. In *Proceedings of the IEEE/CVF Conference on Computer Vision and Pattern Recognition*, pages 1532–1540, 2021. 3
- [31] Yujun Shen, Jinjin Gu, Xiaoou Tang, and Bolei Zhou. Interpreting the latent space of gans for semantic face editing. In *Proceedings of the IEEE/CVF conference on computer vision and pattern recognition*, pages 9243–9252, 2020. 3
- [32] Aliaksandr Siarohin, Stéphane Lathuilière, Sergey Tulyakov, Elisa Ricci, and Nicu Sebe. First order motion model for image animation. In *Conference on Neural Information Processing Systems (NeurIPS)*, 2019. 5
- [33] Attila Szabó, Givi Meishvili, and Paolo Favaro. Unsupervised generative 3d shape learning from natural images. *arXiv preprint arXiv:1910.00287*, 2019. 2
- [34] Omer Tov, Yuval Alaluf, Yotam Nitzan, Or Patashnik, and Daniel Cohen-Or. Designing an encoder for stylegan image manipulation. *arXiv preprint arXiv:2102.02766*, 2021. 1, 2, 5
- [35] Andrey Voynov and Artem Babenko. Unsupervised discovery of interpretable directions in the gan latent space. In *International conference on machine learning*, pages 9786–9796. PMLR, 2020. 3, 7
- [36] Jiajun Wu, Chengkai Zhang, Tianfan Xue, Bill Freeman, and Josh Tenenbaum. Learning a probabilistic latent space of object shapes via 3d generative-adversarial modeling. *Advances in neural information processing systems*, 29, 2016. 2
- [37] Richard Zhang, Phillip Isola, Alexei A Efros, Eli Shechtman, and Oliver Wang. The unreasonable effectiveness of deep features as a perceptual metric. In *Proceedings of the IEEE conference on computer vision and pattern recognition*, pages 586–595, 2018. 6

- [38] Peng Zhou, Lingxi Xie, Bingbing Ni, and Qi Tian.  
Cips-3d: A 3d-aware generator of gans based on  
conditionally-independent pixel synthesis. *arXiv preprint*  
*arXiv:2110.09788*, 2021. 2